

Side Group of Poly(3-alkylthiophene)s Controlled Dispersion of Single-Walled Carbon Nanotubes for Transparent Conducting Film

Wei-Chao Chen,^{†,‡,§,⊥} Hsiang-Ting Lien,[#] Tzu-Wei Cheng,^{||} Chaochin Su,^{||} Cheong-Wei Chong,[†] Abhijit Ganguly,^{‡,†} Kuei-Hsien Chen,^{‡,†} and Li-Chyong Chen^{*,†}

[†]Center for Condensed Matter Science, National Taiwan University, Taipei, 10617, Taiwan

[‡]Institute of Atomic and Molecular Science, Academia Sinica, Taipei, 10617, Taiwan

[§]Engineering and System Science, National Tsing Hua University, Hsinchu, 30012, Taiwan

[⊥]Nano Science and Technology Program, Taiwan International Graduate Program, Academia Sinica and National Tsing Hua University, Hsinchu, 30012, Taiwan

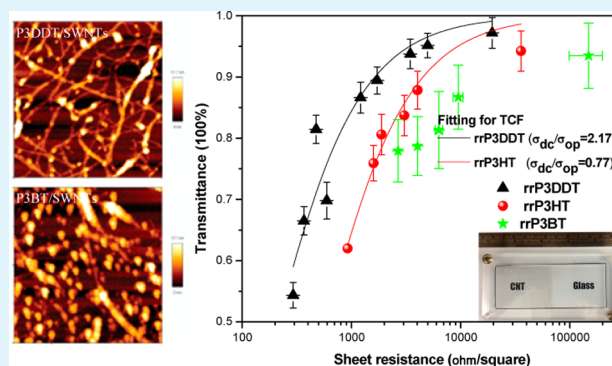
[#]Institute of Polymer Science and Engineering, National Taiwan University, Taipei, 10617, Taiwan

^{||}Department of Molecular Science and Engineering, National Taipei University of Technology, Taipei, 10608, Taiwan

Supporting Information

ABSTRACT: Controlled dispersion of single-walled carbon nanotubes (SWCNTs) in common solvents is a challenging issue, especially for the rising need of low cost flexible transparent conducting films (TCFs). Utilizing conductive polymer as surfactant to facilitate SWCNTs solubility is the most successful pragmatic approach to such problem. Here, we show that dispersion of SWCNT with polymer significantly relies on the length of polymer side groups, which not only influences the diameter distribution of SWCNTs in solution, also eventually affects their effective TCF performance. Surfactants with longer side groups covering larger nanotube surface area could induce adequate steric effect to stabilize the wrapped SWCNTs against the nonspecific aggregation, as discerned by the optical and microscopic measurements, also evidenced from the resultant higher electrokinetic potential. This approach demonstrates a facile route to fabricate large-area SWCNTs-TCFs exhibiting high transmittance and high conductivity, with considerable uniformity over 10 cm × 10 cm.

KEYWORDS: transparent conducting film (TCF), regioregular poly(3-alkylthiophene) (rrP3AT), alkyl side group effect, carbon nanotubes, SWNT dispersion, zeta potential



INTRODUCTION

Advances in optoelectronic devices, namely touch screens, flat panel displays, solar cells, etc., demand the need of transparent electrodes. However, the technology suffers from the cost hidden behind the patterning or designing, and the inherent brittleness of conventional transparent electrodes, such as indium tin oxide (ITO). Recent development in low-cost flexible transparent conducting films (TCFs) using single-walled carbon nanotubes (SWCNTs) offers a potential alternative in optoelectronic device fabrication.^{1–6} In spite of their promising TCFs performances, the issues with the poor dispersion of SWCNTs in common solvents have limited their practical usage.^{7–12} In solution, the van der Waals interactions become exceptionally strong for SWCNTs,^{1,4} which causes the individual nanotubes to naturally align themselves and consequently form large bundles (often referred to as “ropes”). Various methods, such as vacuum filtration,^{13,14} transfer printing,¹⁵ spin-casting,^{5,16} dip-coating,¹⁷ etc., have

been demonstrated to fabricate the carbon nanotube (CNT)-based TCFs. Unfortunately, most of them only promise uniform dispersion in small area, far below the practical scale. Alternative approach such as the rod-and-slot coating technique could overcome such aforementioned drawbacks.¹⁸ However, this method is usually limited by relatively low CNTs concentrations and requirement of covalently linked surface-modifiers, which in turn leads to the presence of nonconducting agents on the nanotube surface.

Utilizing conductive polymer as surfactant to facilitate SWCNTs solubility is one of the most pragmatic approaches to such problem.¹⁹ It is reported that by using conjugated polymers^{20,21} with structures that closely match the surface of the SWCNTs would result in selective solubilization or

Received: November 10, 2014

Accepted: February 10, 2015

Published: February 10, 2015

dispersion of nanotubes not only with selective diameters but also with selective chiral angles. At the same time, the polymer's backbone or side groups favorably wrap around individual SWCNT structures via noncovalent functionalization, while preserving the intrinsic properties of the SWCNTs.²¹ In this work, we show that a significantly improved dispersion of SWCNTs can be achieved by using the regioregular poly-3-alkyl-thiophene (rrP3AT) as a surfactant, via properly selecting the length of rrP3AT side groups. Separation of the well-dispersed SWCNTs from the bundles and amorphous carbon can be achieved via controlled ultracentrifugation process. In principle, by using polythiophene-wrapped SWCNTs (rrP3AT/SWCNTs) dispersed solution; desired quantity of SWCNTs can be coated and sprayed on very large area. Here, we demonstrate a method to fabricate SWCNT TCFs with high transparency and high electrical conductivity, with considerable uniformity on a large glass substrate (10 cm × 10 cm) by ultrasonic spray coating. Our study demonstrates the importance of the side-group-length in polythiophene-based surfactant, which not only benefits the SWCNT dispersion in the solution, but also eventually improves their effective TCFs performance.

METHODS

HiPCo SWCNTs (purity >50%, diameter <1 nm, length <1 μm, was purchased from Carbon Nanotech. Inc. All polymers, including Poly(3-butylthiophene-2,5-diyl), Poly(3-hexylthiophene-2,5-diyl), and Poly(3-dodecylthiophene-2,5-diyl), with molecular weight approximately 45–60 K via GPC and regioregularity 91–94% via NMR, were purchased from Rieke Metal. The solvent, anhydrous Chlorobenzene (99.8%), was purchased from Sigma-Aldrich. The rrP3AT/SWCNTs hybrid solution was prepared by adding 5 mg of HiPCo SWCNTs into appropriate volume of rrP3AT solution to make up a 3% w/v concentration (3 mg of rrP3AT in 100 mL chlorobenzene). According to our initial study, when the relative concentration of SWCNTs in rrP3AT/SWCNTs composites is too low, the sheet resistance of TCF becomes very high because of relatively low conducting polymer dominating the performance. In contrast, for high SWCNTs/polymer ratio, the sheet resistance increases but the transmittance decreases, because of excessive content of amorphous carbon that cannot be ruled out in relatively low rrP3AT concentration level.

The polythiophene we added to stabilize SWCNTs in the chlorobenzene solution have different side groups (-butyl, -hexyl and -dodecyl). Here, we would also like to mention that the P3HT is highly soluble (~50 mg/mL) in chlorinated solvent, such as chlorobenzene, and the P3DDT has even higher solubility than P3HT. Although the solubility of P3BT is relatively low, it still can be totally dissolved in chlorobenzene at such a low concentration (0.03 mg/mL). Therefore, in our case, for all the polymers, irrespective of the side-chain-length, did not show any solubility issue. The solutions were sonicated by using 1/4² probe sonicator operated at 25 W for an optimized time (10 min) in order to exfoliate the bundles of SWCNTs. Longer sonication times did not improve the optical activity of solutions. In order to avoid the temperature influences, during the sonication, the whole sonication system and solution were put into the ice water bath, maintaining the reaction temperature at 0 °C. Subsequently, the well-dispersed SWCNTs centrifuged for 10 min at 12,000 rpm (RCF 16,582 centrifugal force, max) using angle rotor, and the final solution were obtained by decanting the top 90% supernatant.

Transparent Conducting Film Preparation. A predefined quantity of SWCNTs was coated by ultrasonic spray coating with nozzle of 125 mL min⁻¹, with a power supplied at spray-head around 2.5 W. Nitrogen flowing at 2.0 SLPM was used to carry the atomized well-dispersed solution to fabricate the SWCNTs TCFs. The substrate was heated to 150 °C for drying. The as-prepared TCFs were soaked in chlorobenzene for overnight to remove the polymer, and then were placed in 6 M nitric acid for 24 h prior to the characterizations.

Characterizations. Absorbance measurements were taken by using JASCO V 670 UV–visible-near-infrared (UV–vis-NIR) spectrophotometer. The sheet resistance was evaluated by four-point probe technique using silver electrodes, with a correction factor of 4.53 due to small sample thickness. Dynamic light scattering (DLS) measurements were done by using Malvern Zetasizer Nano S to evaluate the hydrodynamic size distribution in solution. Atomic force microscopy (AFM) studies were conducted with JPK NanoWizard II. High-resolution transmission electron microscope (HRTEM) analysis was done with JEOL JEM-2100 field emission TEM operated at 100 kV. Electrokinetic properties were studied to analyze the zeta potential by using Malvern Zetasizer 3000HS.

RESULTS AND DISCUSSION

There have been several literature reports discussing the surfactant effect with molecules of rrP3AT derivatives adsorbed on SWCNTs through π – π interactions.^{20,21} The conjugated thiophene rings adsorbed onto the surface of carbon nanotube similar to that onto HOPG,²² and the interpenetration of the rrP3AT alkyl chains, oriented orthogonal to the backbone, assists the polymer organization.²³ The fact that the length of the side groups would affect the solubility of the polythiophene is well-known. Herein we demonstrate that it could also influence the dispersion nature of polythiophene-wrapped SWCNTs since the rrP3AT with longer side groups could cover larger nanotubes' surface area. In view of this, three kinds of rrP3AT with different side groups were used: poly-3-butylthiophene (rrP3BT, with –C4H9 group), poly-3-hexylthiophene (rrP3HT, having –C6H13 group), and poly-3-dodecylthiophene (rrP3DDT, comprising –C12H25 group). The absorption of rrP3AT is validated in the visible spectral range, while the features observed in the NIR region is attributed to that of SWCNTs (Figure 1). Basically, the optical absorption peak, around 450 nm (Figure 1a), of rrP3AT in chlorobenzene, cannot be observed when rrP3AT interacted with SWCNTs.²⁴ Figure 1a revealed the appearance of vibronic peaks at 550 and 600 nm, for rrP3DDT/SWCNTs. Such vibronic peaks can be observed for all three rrP3AT derivatives, as shown in Figure 1b, suggesting a successful and strong rrP3AT-SWCNTs interaction.²³ Interestingly, very strong SWCNTs-peaks at NIR region can be observed for rrP3DDT/SWCNTs, which provides convincing evidence of well-dispersed SWCNTs with rrP3DDT. In contrast, pure SWCNTs dispersed in chlorobenzene revealed less resolved and low-intensity peaks at NIR region, indicating poor dispersion of unmodified nanotubes. In general, the absorption intensity is proportional to the amount of solubilized nanotubes, independent of whether they are isolated or bundled, while only the semiconducting SWCNTs contributes to the spectral intensity. We can found, in Figure 1b, that all three polymers displayed similar profiles in their absorption spectra, exhibiting similar selective dispersion of SWCNTs. Interestingly, the SWCNTs with longer side groups (rrP3DDT) exhibited the most intense and well-resolved peaks. While the polythiophene derivatives with shorter side groups (rrP3BT and rrP3HT) displayed broader and weaker absorption peaks, which are normally resulted from the agglomeration of SWCNTs, concluding poor SWCNTs-solubility compared to rrP3DDT. The steric effect induced by the longer side groups could be more effective to protect the wrapped SWCNTs against the nonspecific aggregation. Interestingly, as observed in Figure 1b, for the rrP3AT with short side groups, the polythiophene-absorbance intensity was stronger than the SWCNTs-peaks, which also suggests that

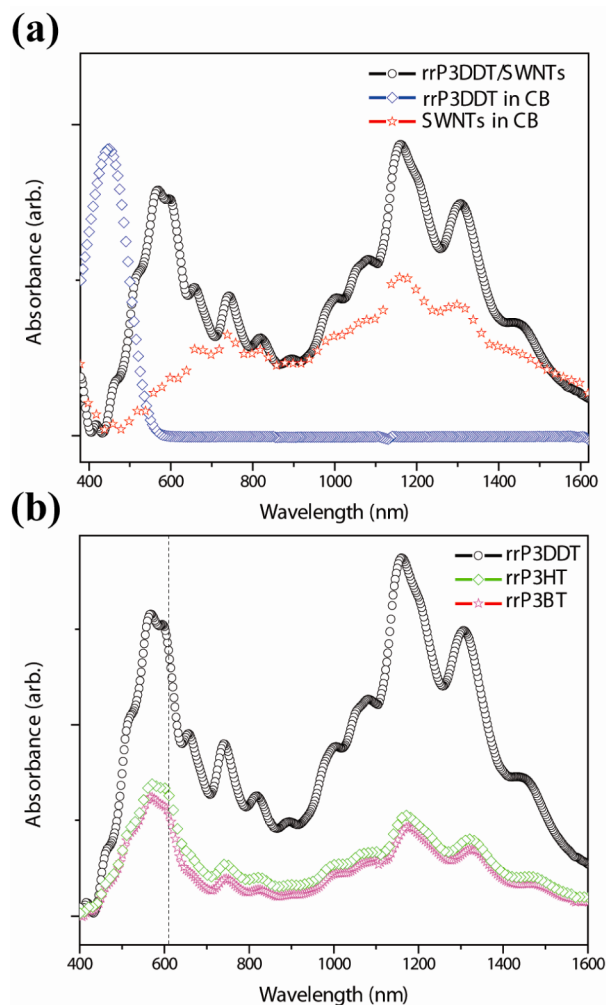


Figure 1. (a) UV-vis-NIR absorption spectra comparing the rrP3DDT/SWCNT dispersion (open circle) with pure SWCNTs (open star) and pure polymer (rrP3DDT, open diamond) in chlorobenzene (CB). (b) Absorption spectra of SWCNTs wrapped with three different polythiophene derivatives in CB solvent: rrP3DDT (open circle), rrP3HT (open diamond), and rrP3BT (open star).

excess polymer content in the respective solution. Therefore, the absorbance study provides important information that the side groups-length of rrP3AT-based surfactant could dominate the SWCNTs dispersion.

Comparative study on the effects of the nature of dispersion for different rrP3AT/SWCNTs composites on their resultant TCFs properties has been performed. Better TCFs properties were observed when polythiophene with longer side groups was used as the surfactant. Major factors that could improve the TCFs performance include the reduction of bundle-diameter, junction-density, and doping. As shown in Figure 2, the TCFs conductivity is improved as the side groups of polythiophene are lengthened. Accordingly, the TCFs derived from rrP3DDT-wrapped SWCNTs exhibits a sheet resistance (R_s) of $\sim 390 \Omega$ at 80% transmittance (T) in visible regime, compared with the R_s of $>1000 \Omega$ and $>5000 \Omega$ for the TCFs deposited by SWCNTs wrapped by rrP3HT and rrP3BT, respectively, at the same transmittance, T . The electron transport in SWCNTs networks could be hindered by the junction-resistance,¹⁹ which increases as the size of interconnecting bundle increases. In line with this, we can predict that the SWCNTs wrapped with

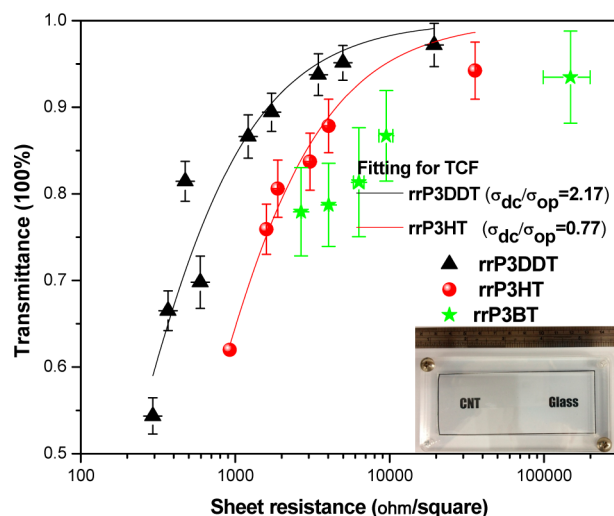


Figure 2. Performance of SWCNT-based transparent conducting films (TCFs) fabricated by using rrP3AT surfactant with different side groups. Inset: Optical photograph of TCF prepared on cut 10 cm \times 10 cm soda lime glass.

polymer having shorter side groups (rrP3BT or rrP3HT) suffer from serious aggregation and formation of large bundles, thus resulting in poor conductivity. For TCFs having thicknesses lower than 100 nm, which is considerably shorter than the wavelengths in Vis-NIR regime, the R_s can be related to T at a given wavelength as follows:²⁵

$$T = \left(1 + \frac{1}{2R_s} \sqrt{\frac{\mu_0}{\epsilon_0}} \frac{\sigma_{op}}{\sigma_{dc}} \right)^{-2} = \left(1 + \frac{188(\Omega)}{R_s} \frac{\sigma_{op}}{\sigma_{dc}} \right)^{-2}$$

where σ_{op} is the optical conductivity which varies as a function of wavelength; σ_{dc} is the direct current conductivity. The μ_0 ($4\pi \times 10^{-7} \text{ s}^2/\text{F}\cdot\text{m}$) and ϵ_0 ($8.85 \times 10^{-12} \text{ F/m}$) are the permeability and permittivity of free space, respectively. This equation was used to fit the measured transmittance data as shown in Figure 2. The electronic properties of SWCNTs are very important for TCF application, at the same time their optical properties also need to be considered. The transmittance, T , of a thin film can be related to the optical conductivity, σ_{op} , just like the sheet resistance, R_s , related to σ_{dc} . Therefore, the conductivity ratio of σ_{dc}/σ_{op} can be treated as a figure of merit, which correlates the T and the R_s . The σ_{dc}/σ_{op} ratio represents an overall evaluation of the optoelectronic properties of TCF, and the higher ratios symbolize better optoelectronic properties. The rrP3AT/SWCNTs-based TCFs showed a clear reduction in R_s when the SWCNTs were dispersed with longer side-group polymers (rrP3DDT). Such improvement can be quantified by extracting σ_{dc}/σ_{op} ratio from the fitting parameter. For the rrP3HT/SWCNTs TCFs, the average value of σ_{dc}/σ_{op} was found to be closed to 0.77, over visible wavelengths from 300 to 1100 nm, whereas the σ_{dc}/σ_{op} has increased to 2.2 for the films of SWCNTs wrapped with rrP3DDT. This leads us to think that the variation in rrP3AT side groups can influence the dispersion of SWCNTs in solution, consequently the resultant TCFs performance.

Effect of the side-group-length of rrP3AT on the diameter distribution of SWCNTs in solution can be observed from the dynamic light scattering (DLS) measurements. Figures 3a revealed mainly two narrow Gaussian distributions of the hydrodynamic size of SWCNTs, wrapped with rrP3DDT: one

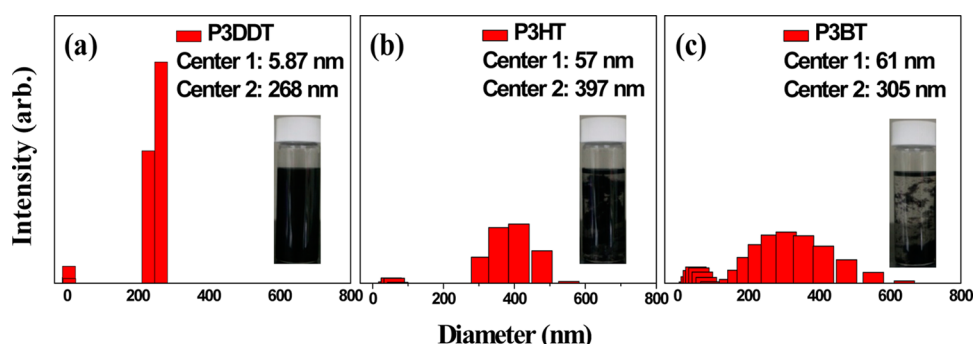


Figure 3. DLS results revealing the size distribution of the polymer-wrapped SWCNT in solution: (a) rrP3DDT/SWCNTs, (b) rrP3HT/SWCNT, and (c) rrP3BT/SWCNT composites. Center 1 and 2 specify the average diameter and length of the composites, respectively. Inset photographs representing the 2 week stability test of the corresponding rrP3AT/SWCNTs composites.

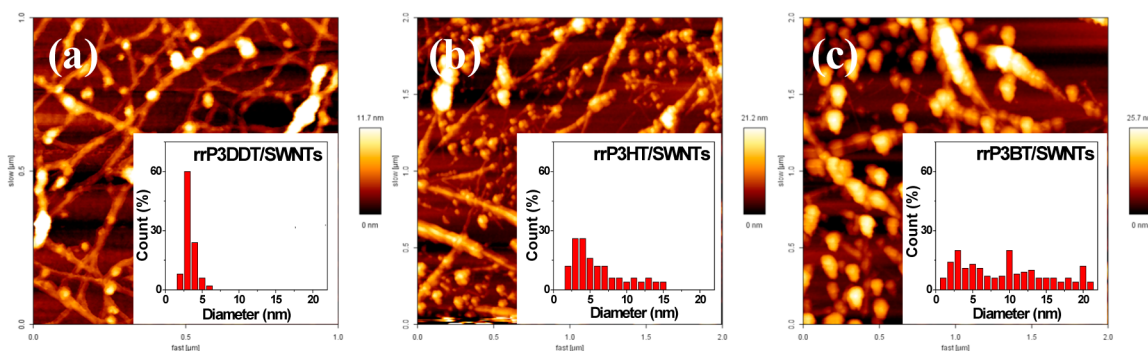


Figure 4. AFM images of the SWCNTs based TCFs fabricated by using polythiophene surfactant with different side groups: (a) rrP3DDT, (b) rrP3HT and (c) rrP3BT. Inset figures correspond to the diameter distribution of the rrP3AT/SWCNTs composites.

centered around 5.87 nm (Center 1) and the other at ~ 268 nm (Center 2). The peak with lower size-distribution could be attributed to the diameter of nanodispersed SWCNTs, while the second peak at higher range represents the length of dispersed composites.¹² Presence of these peaks can be approximated to the alignment of bundle and individual nanotube to the polarization direction of incident laser beam.²⁴ The SWCNTs wrapped with the shortest side-group polythiophene (rrP3BT) exhibited severe broadening for both the peaks, suggesting a significant bundle formation (Figure 3c). On the contrary, the peak-widths reduced extremely as SWCNT interacted with longer side-group dispersant (Figure 3b to 3a); especially with rrP3DDT (Figure 3a), referring to the well dispersion of individual nanotubes. The observed nanodispersion phenomenon can easily be achieved due to the steric effect induced by long dodecyl-groups of rrP3DDT within two adjacent nanotubes.²⁵ However, rrP3BT and rrP3HT, with short butyl and hexyl groups, respectively, cannot provide sufficient repulsive force to overcome the van der Waals force between the nanotubes, finally leading to a profuse nanotube aggregation and subsequent bundle formation. To test the stability of the wrapped SWCNT dispersion in solution, we left all three polymer-wrapped SWCNTs solutions standing in three separate vials, in nonturbulent environment. After 2 weeks, the SWCNTs wrapped with shorter side group polymers (rrP3BT and rrP3HT) were found to be precipitated in solution, shown in Figure 3c and 3b (insets), respectively, whereas the rrP3DDT/SWCNTs could retain the uniform dispersion nature (inset, Figure 3a).

The DLS technique is a reciprocal method, the measurement on individual nanotubes with a few-nanometer size would be constrained by the resolution limit of the operating system. The

diameter of as-purchased SWCNTs is closed to 1 nm and expected to increase by several angstroms with polymer-wrapping around the tubes. In order to check the reliability of the DLS results, we have performed atomic force microscopy (AFM) study on various polythiophene-wrapped SWCNTs spin-coated on polished silicon substrates. The rrP3DDT/SWCNTs composites showed good distribution of nanodispersed and uniformly wrapped SWCNTs network (Figure 4a). Noticeably, few spherical (ball-like) and elliptical (corn-like) thicker structures can be observed sticking on the SWCNTs network. The shapes and sizes of these thicker features can be evidently distinguished from the long 1D nanostructures of polymer/SWCNTs composites. These thicker features were also profusely broadened and increased, both in number density and size distribution, as the length of rrP3AT side groups decreased (as evidenced from the colored height-scale bar shown besides the Figure 4b, c). Moreover, as the rrP3AT chains are shortened, there is a drastic reduction of long nanotube structures observed: the composite of SWCNTs with rrP3BT exhibited the extreme condition. Here, it should be noted that the scanning area for rrP3DDT-based composites (Figure 4a) is half of those shown in Figure 4b, c, for shorter side-chain polymers (rrP3BT and rrP3HT). It has been reported earlier²⁶ that the adsorption and folding of polythiophene molecules like rrP3HT on individual SWCNTs is a relatively fast phenomenon, which would complete at very initial stage. Subsequently, the strong correlation between the SWCNTs and rrP3AT dynamics results to the formation of small bundles of SWCNTs, and the excess addition of rrP3AT would form the all-polythiophene domains. The situation would be profoundly obvious for the rrP3AT with shorter side groups, as realized from the ball- and-corn-like thicker

structures observed in Figures 4b, c. Such formation of the pure-polythiophene domains can also be realized from the stronger rrP3AT-absorbance intensity relative to the SWCNT peaks, as observed in the UV-vis-NIR absorption spectra for rrP3HT and rrP3BT (Figure 1b). However, such pure-polymer domain formation is less possible for rrP3DDT, mainly attributed to the preferred adsorption of long-chained molecules on CNTs over the shorter-chained ones. Such preference has been established earlier²⁷ and also suggested to be contributed by the enhanced adsorption energy with more binding sites and less edge effects for the longer-chain molecules. Moreover, the rrP3DDT/SWCNTs revealed much narrower diameter distribution of nanotube-composites centered around 3 nm (inset, Figure 4a), in contrast to the other two polythiophene derivatives, which is also consistent with the DLS results. From the diameter distribution plots (insets, Figure 4b, c), we can conclude that the dispersion of SWCNTs with shorter side groups surfactants would easily result in mixed bundles composites and all-polythiophene domain formation, which in turn would reduce the effective number of rrP3AT/SWCNTs composites.

Although AFM studies clearly revealed different polymerized phenomena for nanotubes decorated with different side groups, the polymer-wrapping state is vividly appeared in the high-resolution transmission electron microscopic (HRTEM) images (Figure 5). The image of rrP3DDT/SWCNTs (Figure

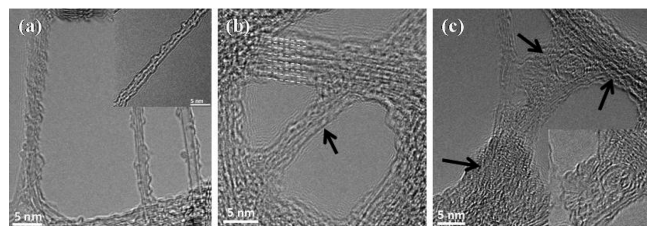


Figure 5. TEM images of polythiophene/SWCNTs composites: (a) rrP3DDT, (b) rrP3HT, and (c) rrP3BT. Black arrows indicate the polymer domain and bundled structures. The inset of a indicates single helical wrapped rrP3DDT/SWCNTs composite, and the inset of c indicates the polymer domain region.

5a) clearly shows a typical helical wrapping composite structure (inset of Figure 5a), indicating the presence of single SWCNTs (or very thin bundle of at most 2–3 SWCNTs), with the diameter distribution close to 1.3 nm (Figure 5d and Supporting Information, Figure S1a). However, the SWCNTs wrapped with shorter side groups revealed much thicker bundles (Figure 5b, c), with an extreme condition for rrP3BT (with 7–10 SWCNTs in each bundle), indicating serious aggregation effect. From these TEM observations, it is quite obvious that the outer surface of the bundled rrP3AT/SWCNTs composite is polymer-rich, and for shorter chained polythiophene (especially, rrP3BT), we can observe pure-polymer domains (Figure 5c, inset), similar to those observed in AFM image (Figure 4c).

Electrokinetic or zeta potential (ζ) of a colloidal system is a useful parameter in understanding the dispersion behavior of colloids,^{4,28} assessing the degree of colloidal stability and the particle-interaction in solution. In earlier reports,^{29,30} the CNTs Fermi level was suggested to be blue-shifted with respect to the polythiophene attached on the nanotube sidewalls, resulting in a large built-in potential that could attribute to a significant amount of charge-transfer from the polythiophene sulfur atoms to the CNTs in the ground state.^{31,32} Because the charge transfer occurs between the polythiophene and SWCNTs once the rrP3AT starts to wrap the SWCNTs, there must be an induced electrical potential gradient existing at the SWCNT–polymer interface, resulting in a measurable surface potential and hence the ζ values for the rrP3AT/SWCNTs system. From our study, we have also observed that the measured ζ value is entirely contributed by the rrP3AT/SWCNTs composites (Supporting Information, Figure S2). Pure rrP3AT or pure SWCNTs solution could not show any significant ζ values, which would consecutively suggest that the presence of bundled or heavily agglomerated nanotubes or all-polythiophene domains would lower the induced surface potential, and hence the effective ζ value. The hypothesis can be justified while an increase in ζ from 39.3 mV to 100.3 mV was observed with the increase in the length of rrP3AT side groups, as observed in Figure 6a, which signifies a good correlation to our earlier claims.

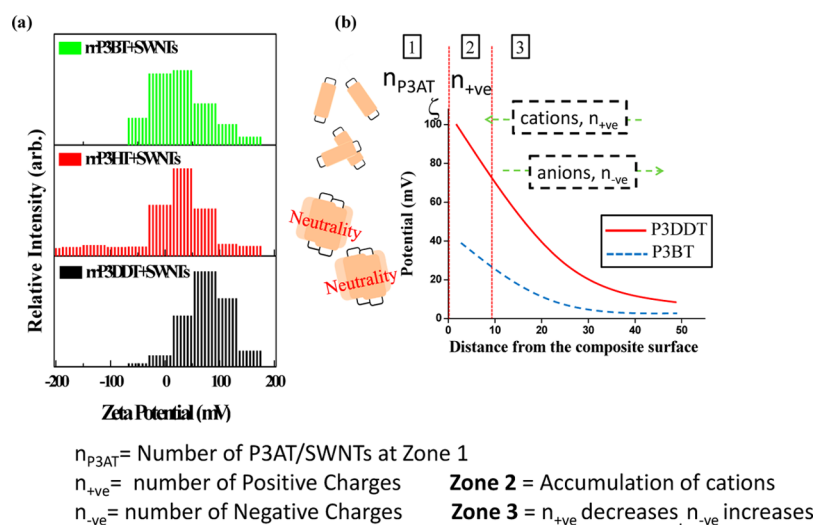


Figure 6. (a) Zeta potential (ζ) distribution comparing different rrP3AT-wrapped SWCNTs. (b) Schematic illustration of the surface potential change revealing the effect of the side-chain-length of rrP3AT-based surfactant.

Inevitably, the films of SWCNTs wrapped by shorter side groups rrP3AT, exhibiting severe agglomeration of SWCNTs and excess all-polythiophene domains, possess lower ζ value because of the loss in the effective number of individual rrP3AT/SWCNTs composites, which is conceptually depicted in Figure 6b. Therefore, we can conclude that the side-group length of the surfactant not only influences the rrP3AT/SWCNTs distribution in solution but also eventually affects their effective electrokinetic behavior. There is a possibility that different chain lengths of P3AT can provide different energy level differences against SWCNTs, which can further affect the induced charge transfer and hence the resultant ζ value. However, earlier studies have shown that there is no significant effect of alkyl side-chain length of polymer on its HOMO/LUMO energy levels.^{31,32} Therefore, the differences in ζ values would mainly be governed by the aggregation phenomenon happening in chlorobenzene solution. As we have mentioned earlier, the adsorption of long-chained molecules on CNTs is preferable to that of shorter-chained ones,²⁷ and this adsorption process, being a relatively fast phenomenon, would complete at the very initial stage.²⁶ Hence, the treatment with short-chained molecules like rrP3BT would easily result in all-polythiophene domains with SWCNT bundles formation, reducing the effective number of nanodispersed rrP3AT/SWCNTs composites. Even though, we have observed an extreme difference in nanodispersion results between rrP3DDT and rrP3BT, it is still difficult, at this stage, to clarify the exact reason(s) behind such large change in ζ values depending on the chain length of rrP3AT. It is also difficult to account the exact contribution of the induced electrical potential gradient; here we can report only our experimental observations. Nevertheless, we believe these results could stimulate further study/research on the charge transfer phenomenon between SWCNTs and rrP3AT, as well as their carrier dynamics, which would supplement the information contained herein.

Lastly, regarding the TCFs performance as presented in Figure 2, it should be mentioned that, compared to our work, several groups³ have reported a superior TCF property of their SWCNT-based TCFs, utilizing longer arc-discharge SWCNTs (5–20 μm) with higher purity of about 60–70%. Unfortunately, we were not able to access such high-quality SWCNTs. In the present work, the SWCNTs that we used are shorter in length (<1 μm) and lower in purity (~50%). Furthermore, some groups have also performed certain purification steps and a complicated doping process (use of SOCl_2)^{3–5} in order to lower the junction resistance and defect density, and further improve the TCFs-performances. Here, the only post-treatment we did was the nitric acid treatment in order to achieve an effective removal of surfactant, and thus form nanotube–nanotube junctions.²³ Nonetheless, here, our main objective was to establish the importance of side-chain length of the surfactants for both the SWCNT dispersion and the final TCFs performances. We believe that the ultimate performance can be enhanced further by improving the material qualities as well as optimizing the fabrication process.

CONCLUSIONS

We have demonstrated the effect of polythiophene derivatives with different side groups as surfactant for the dispersion of SWCNTs. The dispersed nanotubes were subsequently coated on the glass substrate in order to assess its performance as transparent conducting film. The study showed that as the rrP3AT side groups lengthen the fabricated TCFs show better

transparency and conductivity. In this work, the rrP3DDT/SWCNTs exhibits the best performance because of the effectiveness of the long alkyl chain length that can induce adequate steric effect to stabilize the wrapped SWCNTs against the nonspecific aggregation. By minimizing the bundled and cornlike networks (nanotube aggregates), we can effectively reduce the junction resistance and improve the final TCFs performance.

ASSOCIATED CONTENT

Supporting Information

Large-area TEM images and the zeta potential of both pure rrP3AT and pure SWCNTs solution are shown here. This material is available free of charge via the Internet at <http://pubs.acs.org>.

AUTHOR INFORMATION

Corresponding Author

*E-mail: chenlc@ntu.edu.tw.

Notes

The authors declare no competing financial interest.

ACKNOWLEDGMENTS

This research was financially supported by the Ministry of Education, Ministry of Science and Technology, Academia Sinica (Taiwan), TIGP Academia Sinica program, and Asian Office of Aerospace Research and Development under AFOSR. Technical support was provided by the Core Facilities for Nano Science and Technology, Academia Sinica, and National Taiwan University.

REFERENCES

- (1) Cao, Q.; Rogers, J. A. Ultrathin Films of Single-Walled Carbon Nanotubes for Electronics and Sensors: A Review of Fundamental and Applied Aspects. *Adv. Mater.* **2009**, *21*, 29–53.
- (2) Feng, C.; Liu, K.; Wu, J. S.; Liu, L.; Cheng, J. S.; Zhang, Y.; Sun, Y. H.; Li, Q. Q.; Fan, S. S.; Jiang, K. L. Flexible, Stretchable, Transparent Conducting Films Made from Super Aligned Carbon Nanotubes. *Adv. Funct. Mater.* **2010**, *20*, 885–891.
- (3) Geng, H. Z.; Kim, K. K.; So, K. P.; Lee, Y. S.; Chang, Y.; Lee, Y. H. Effect of Acid Treatment on Carbon Nanotube-Based Flexible Transparent Conducting Films. *J. Am. Chem. Soc.* **2007**, *129*, 7758–7759.
- (4) Hu, L.; Hecht, D. S.; Grüner, G. Carbon Nanotube Thin Films: Fabrication, Properties, and Applications. *Chem. Rev.* **2010**, *110*, 5790–5844.
- (5) Jo, J. W.; Jung, J. W.; Lee, J. U.; Jo, W. H. Fabrication of Highly Conductive and Transparent Thin Films from Single-Walled Carbon Nanotubes Using a New Non-Ionic Surfactant via Spin Coating. *ACS Nano* **2010**, *4*, 5382–5388.
- (6) Tenent, R. C.; Barnes, T. M.; Bergeson, J. D.; Ferguson, A. J.; To, B.; Gedvilas, L. M.; Heben, M. J.; Blackburn, J. L. Ultrasoft, Large-Area, High-Uniformity, Conductive Transparent Single-Walled-Carbon-Nanotube Films for Photovoltaics Produced by Ultrasonic Spraying. *Adv. Mater.* **2009**, *21*, 3210–3216.
- (7) Chen, F.; Wang, B.; Chen, Y.; Li, L. J. Toward the Extraction of Single Species of Single-Walled Carbon Nanotubes Using Fluorene-Based Polymers. *Nano Lett.* **2007**, *7*, 3013–3017.
- (8) Hersam, M. C. Progress Towards Monodisperse Single-Walled Carbon Nanotubes. *Nat. Nanotechnol.* **2008**, *3*, 387–394.
- (9) Lou, X. W.; Archer, L. A.; Yang, Z. Hollow Micro-/Nanostructures: Synthesis and Applications. *Adv. Mater.* **2008**, *20*, 3987–4019.
- (10) Shin, H. J.; Kim, S. M.; Yoon, S.-M.; Benayad, A.; Kim, K. K.; Kim, S. J.; Park, H. K.; Choi, J. Y.; Lee, Y. H. Tailoring Electronic

Structures of Carbon Nanotubes by Solvent with Electron-Donating and-Withdrawing Groups. *J. Am. Chem. Soc.* **2008**, *130*, 2062–2066.

(11) Tu, X.; Manohar, S.; Jagota, A.; Zheng, M. DNA Sequence Motifs for Structure-Specific Recognition and Separation of Carbon Nanotubes. *Nature* **2009**, *460*, 250–253.

(12) Zheng, M.; Jagota, A.; Semke, E. D.; Diner, B. A.; McLean, R. S.; Lustig, S. R.; Richardson, R. E.; Tasset, N. G. DNA-Assisted Dispersion and Separation of Carbon Nanotubes. *Nat. Mater.* **2003**, *2*, 338–342.

(13) Wu, Z.; Chen, Z.; Du, X.; Logan, J. M.; Sippel, J.; Nikolou, M.; Kamaras, K.; Reynolds, J. R.; Tanner, D. B.; Hebard, A. F.; Rinzler, A. G. Transparent, Conductive Carbon Nanotube Films. *Science* **2004**, *305*, 1273–1276.

(14) Hou, P. X.; Yu, B.; Su, Y.; Shi, C.; Zhang, L. L.; Liu, C.; Li, S. S.; Du, J. H.; Chenget, H. M. Double-Wall Carbon Nanotube Transparent Conductive Films with Excellent Performance. *J. Mater. Chem. A* **2014**, *2*, 1159–1164.

(15) Dan, B.; Irvin, G. C.; Pasquali, M. Continuous and Scalable Fabrication of Transparent Conducting Carbon Nanotube Films. *ACS Nano* **2009**, *3*, 835–843.

(16) Kim, S.; Yim, J.; Wang, X.; Bradley, D. D. C.; Lee, S.; deMello, J. C. Spin and Spray Deposited Single Walled Carbon Nanotube Electrodes for Organic Solar Cells. *Adv. Funct. Mater.* **2010**, *20*, 2310–2316.

(17) Peng, K.; Liu, L. Q.; Gao, Y.; Qu, M. Z.; Zhang, Z. Fabrication of High Optical Transparent and Conductive SWNT Based Transparent Conducting Film on Flexible Plastic Substrate Using Ozone as a Redox Dopant. *J. Nanosci. Nanotechnol.* **2010**, *10*, 7386–7389.

(18) Rowley, L.; Irvin, G.; Anderson, C.; Majumdar, D. Coating Compositions Containing Single Wall Carbon Nanotubes. *US patent* 2006/0188723 A1, 2006.

(19) Yang, S. B.; Kong, B. S.; Jung, D. H.; Baek, Y. K.; Han, C. S.; Oh, S. K.; Jung, H. T. Recent Advances in Hybrids of Carbon Nanotube Network Films and Nanomaterials for Their Potential Applications as Transparent Conducting Films. *Nanoscale* **2011**, *3*, 1361–1373.

(20) Hwang, J. Y.; Nish, A.; Doig, J.; Douven, S.; Chen, L. C.; Nicholas, R. J. Polymer Structure and Solvent Effects on the Selective Dispersion of Single-Walled Carbon Nanotubes. *J. Am. Chem. Soc.* **2008**, *130*, 3543–3553.

(21) Nish, A.; Hwang, J. Y.; Doig, J.; Nicholas, R. J. Highly Selective Dispersion of Single-Walled Carbon Nanotubes Using Aromatic Polymers. *Nat. Nanotechnol.* **2007**, *2*, 640–646.

(22) Mena-Osteritz, E. Superstructures of Self-Organizing Thiophenes. *Adv. Mater.* **2002**, *14*, 609–616.

(23) Giulianini, M.; Waclawik, E. R.; Bell, J. M.; Crescenzi, M. D.; Castrucci, P.; Scarselli, M.; Motta, N. Poly(3-hexyl-thiophene) Coil-Wrapped Single Wall Carbon Nanotube Investigated by Scanning Tunneling Spectroscopy. *Appl. Phys. Lett.* **2009**, *95*, 013304–013303.

(24) Lee, H. W.; Yoon, Y.; Park, S.; Oh, J. H.; Hong, S.; Liyanage, L. S.; Wang, H. L.; Morishita, S.; Patil, N.; Park, Y. J.; Park, J. J.; Spakowitz, A.; Galli, G.; Gygi, F.; Wong, P. H. S.; Tok, J. B. H.; Kim, J. M.; Baoet, Z. Selective Dispersion of High Purity Semiconducting Single-Walled Carbon Nanotubes with Regioregular Poly(3-alkylthiophene)s. *Nat. Commun.* **2011**, *2*, 541.

(25) Nirmalraj, P. N.; Lyons, P. E.; De, S.; Coleman, J. N.; Boland, J. J. Electrical Connectivity in Single-Walled Carbon Nanotube Networks. *Nano Lett.* **2009**, *9*, 3890–3895.

(26) Lee, J. Y.; Kim, J. S.; Hyeok, K. A.; Lee, K.; Kim, D. Y.; Bae, D. J.; Lee, Y. H. Electrophoretic and Dynamic Light Scattering in Evaluating Dispersion and Size Distribution of Single-Walled Carbon Nanotubes. *J. Nanosci. Nanotechnol.* **2005**, *5*, 1045–1049.

(27) Shvartzman-Cohen, R.; Nativ-Roth, E.; Baskaran, E.; Levi-Kalishman, Y.; Szeifer, I.; Yerushalmi-Rozen, R. Selective Dispersion of Single-Walled Carbon Nanotubes in the Presence of Polymers: the Role of Molecular and Colloidal Length Scales. *J. Am. Chem. Soc.* **2004**, *126*, 14850–14857.

(28) Bernardi, M.; Giulianini, M.; Grossman, J. C. Self-Assembly and its Impact on Interfacial Charge Transfer in Carbon Nanotube/P3HT Solar Cells. *ACS Nano* **2010**, *4*, 6599–6606.

(29) Wei, C. Adsorption of an Alkane Mixture on Carbon Nanotubes: Selectivity and Kinetics. *Phys. Rev. B* **2009**, *80*, 085409.

(30) White, B.; Banerjee, S.; O'Brien, S.; Turro, N. J.; Herman, I. P. Zeta-Potential Measurements of Surfactant-Wrapped Individual Single-Walled Carbon Nanotubes. *J. Phys. Chem. C* **2007**, *111*, 13684–13690.

(31) Geng, J.; Zeng, T. Influence of Single-Walled Carbon Nanotubes Induced Crystallinity Enhancement and Morphology Change on Polymer Photovoltaic Devices. *J. Am. Chem. Soc.* **2006**, *128*, 16827–16833.

(32) Kanai, Y.; Grossman, J. C. Role of Semiconducting and Metallic Tubes in P3HT/Carbon-Nanotube Photovoltaic Heterojunctions: Density Functional Theory Calculations. *Nano Lett.* **2008**, *8*, 908–912.